Diabetes Technology and Therapeutics

DOI: 10.1089/dia.2020.0110

The Padova Type 2 Diabetes Simulator from Triple-Tracer Single Meal Studies: *In Silico* Trials also possible in Rare but Not-So-Rare Individuals

Roberto Visentin, PhD[1], Claudio Cobelli, PhD[1], Chiara Dalla Man, PhD[1]

(1) Department of Information Engineering, University of Padova, Padova, Italy

Word count (max 5000, core): 4579 (including References and Appendix)

Running title (max 45 characters): The Padova Type 2 Diabetes Simulator

N° Figures/Tables: 6 (Figures) + 2 (Tables)

Search Items (3 to 6): simulation, physiological control, glucose metabolism, insulin secretion, insulin action, model identification

Funding source: This work supported by MIUR (Italian Minister for Education) under the initiative “Departments of Excellence” (Law 232/2016) and CARIPARO (Cassa di Risparmio di Padova e Rovigo) foundation under the initiative “Pediatric Research 2016-2018” (BCPD project).

Corresponding Author:

Prof. Claudio Cobelli,

Department of Information Engineering,

University of Padova, Via Gradenigo 6/B,

I-35131 Padova, Italy

Tel: 39-049-8277661

Fax: 39-049-8277699

e-mail: cobelli@dei.unipd.it

Diabetes Technology and Therapeutics
The Padova Type 2 Diabetes Simulator from Triple-Tracer Single Meal Studies: In Silico Trials also possible in Rare but Not-So-Rare Individuals (DOI: 10.1089/dia.2020.0110)

ABSTRACT

Background: *In silico* trials in type 2 diabetes (T2D) would be useful for testing diabetes treatments and accelerating the development of new antidiabetic drugs. Here we present a T2D simulator able to reproduce the variability observed in a T2D population. The simulator also allows to safely experimenting on virtual subjects with severe (and possibly rare) pathological conditions.

Methods: A meal simulation model of glucose, insulin and C-peptide systems, made of 15 differential equations and 39 parameters, has been identified using a system decomposition and forcing function Bayesian strategy on data of 51 T2D subjects undergoing a single triple-tracer mixed meal. One hundred T2D *in silico* subjects have been generated from the joint distribution of estimated model parameters. A case study is presented to illustrate the simulator use for testing a virtual drug (improving insulin action and secretion) in a subpopulation of rare, extremely impaired, T2D subjects.

Results: The model well fitted T2D data and parameters were estimated with precision. Simulated plasma glucose, insulin and C-peptide well matched the data (e.g., median [25^{th}-75^{th} percentile] glucose AUC of 6.9 [6.1-8.5] 10^4 mg/dL·min *in silico* vs. 7.0 [5.6-8.2] 10^4 mg/dL·min *in vivo*). The potential use of the simulator was shown in a case study, in which the (virtual) antidiabetic drug dose was optimized for very insulin-resistant T2D subjects.

Conclusions: We have developed a T2D simulator that captures the behavior of T2D population during a meal, both in terms of average and inter-subject variability. The simulator represents a cost-effective way to test new antidiabetic drugs, before moving to human trials.

Diabetes Technology and Therapeutics
The Padova Type 2 Diabetes Simulator from Triple-Tracer Single Meal Studies: In Silico Trials also possible in Rare but Not-So-Rare Individuals (DOI: 10.1089/dia.2020.0110)

INTRODUCTION

In Silico Clinical Trials (ISCT) are defined as "The use of individualized computer simulation in the development or regulatory evaluation of a medicinal product, medical device, or medical intervention" [1]. They aim to recreate the concept of *in vivo* trials using an *in silico* approach, where a large number of individual patients is modeled by initializing a disease/intervention model. As discussed in [1], realistic ISCTs necessitate the availability of a cohort of *in silico* "subjects" spanning the variability observed in the study population, i.e. an average model is useless.

In type 1 diabetes (T1D), *in silico* experiments have been of enormous value to accelerate technology development, e.g. subcutaneous glucose sensors, novel insulin molecules and the artificial pancreas, thanks to the availability of the U.S. Food and Drug Administration (FDA) accepted UVA/Padova T1D simulator [2]-[4], which allows a time- and cost-effective alternative to preclinical studies, (e.g., [5]-[14]).

However, among the almost 500 million people in the world having diabetes, only 10-15% has T1D. The vast majority are subjects with type 2 diabetes (T2D). These patients are often treated with medications to control their blood glucose levels: some of these medications are orally administered (e.g., biguanides, sulfonylureas, Dipeptidyl Peptidase 4 inhibitors) [15], some others are given by injection (e.g., insulin, amylin analogues, Glucagon-Like Peptide-1 receptor agonists) [16]. Testing new treatments or combination of medications is time consuming and expensive. Therefore, a simulator to perform ISCT in T2D would be highly desirable.

Here, we develop a single meal T2D simulator using a data base of 51 T2D subjects [17]-[19], studied with the triple-tracer meal technique [20]. This technique provides the main glucose fluxes in the body (i.e. meal rate of appearance, endogenous production, and peripheral utilization) in a virtually model-independent way, which, together with plasma glucose, insulin and C-peptide concentrations measured during the meal, allow to accurately estimate the T2D model parameters, and thus their distributions. A case study is also provided to show the potential use of the simulator for optimal drug design in rare, but not so rare, T2D individuals, e.g., subjects with severely impaired insulin secretion and/or action.

RESEARCH DESIGN & METHODS

Database and Protocol

We used data of 51 T2D subjects (Age=54.6±8.5 years, BW=94.1±15.5 kg, BMI=33.1±5.5 kg/m^2) [17]-[19]. Subjects underwent a triple-tracer mixed meal test [20] with different carbohydrate (CHO) content (75 g per subject in [17], 75±2 g per subject in [18], and 1.2 g/kg per subject in [19], respectively). [1-^{13}C]glucose tracer was added to the meal, while [6,6-$^2H_2$]glucose and [6-^{3}H]glucose were intravenously infused to mimic the endogenous glucose production (*EGP*) and the meal glucose rate of appearance (Ra_{meal}), respectively. Glucose concentrations were measured using a glucose oxidase method (Yellow Springs Instruments, Yellow Springs, OH), while plasma insulin was assessed by a chemiluminescence assay with reagents (Access Assay; Beckman, Chaska, MN), and plasma C-peptide by radioimmunoassay using reagents supplied by Linco Research (St. Louis, MO). The triple tracer technique [20] allowed to obtain virtually model-independent estimates of Ra_{meal} and *EGP*. The rate of glucose utilization by the tissues (*U*) was then calculated using estimated Ra_{meal} and *EGP* and the mass balance principle. Fig. 1 reports the mean ± standard deviation (SD) of measured plasma glucose, insulin and C-peptide concentrations, Ra_{meal}, *EGP* and *U* in T2D subjects. We refer to [17]-[19] for a more detailed description of the measurement techniques.

For purpose of comparison, we also used a database of 204 healthy subjects (H, Age=56.5±21.7 years, BW=78.0±13.3 kg, BMI=26.6±3.4 kg/m^2) undergoing a triple-tracer mixed meal test with 1.2 CHO g/kg [21].

The Model

A scheme of the model describing the glucose-insulin interaction in T2D subjects is shown in Fig. 2. The complete list of model equations and the meaning of the model parameters are reported in the Appendix for reader convenience. For further details on the model, we refer to [22]-[24].

Briefly, the model derives from that proposed by Dalla Man and colleagues in 2007 [22]. Like the original model, this one describes the glucose transit through the gastro-intestinal tract, the action of insulin on glucose utilization and endogenous production, and the control of glucose on insulin secretion. The glucose subsystem is described by a two-compartment model [22]: insulin-independent utilization occurs in the first compartment,

representing plasma and rapidly equilibrating tissues, while insulin-dependent utilization occurs in a remote compartment, representing peripheral tissues. At variance with [22], a three-compartment model is used to describe insulin kinetics in the liver (I_l), in the plasma (I_p), and in extravascular space (I_{ev}) [23],[24]. A two-compartment model is also added to describe C-peptide kinetics [25],[26].

Metabolic fluxes accounted in the model are *EGP*, Ra_{meal}, *U*, β-cell insulin secretion rate (*ISR*), and hepatic insulin extraction (*HE*). *EGP* suppression is assumed to be linearly dependent on plasma glucose, liver insulin, and a delayed plasma insulin signal [27]; one of the key model parameters is hepatic insulin sensitivity (k_{p3}), which quantifies insulin control on *EGP* suppression. Ra_{meal} is described with a three compartment model, two representing the stomach (solid and triturated compartments), and one the gut [28]. Glucose utilization (*U*) is made up of two components: insulin-independent utilization (U_{ii}) in the brain and erythrocytes is assumed constant, while insulin-dependent utilization (U_{id}) in muscle and adipose tissues depends nonlinearly (Michaelis–Menten) from glucose in the tissues [29]; one of the key model parameters is disposal insulin sensitivity (V_{mx}). The model also assumes that, when glucose decreases below its basal value, a paradoxical increase in insulin sensitivity occurs, as previously described [3]. *ISR* is assumed to be made of a basal, a dynamic and a static component, and modeled as in [25],[26]: the dynamic component represents the release of promptly releasable insulin and is proportional to the rate of increase of glucose concentration through a parameter called dynamic β-cell responsivity (Φ_d); the static component describes the provision of new insulin to the releasable pool and is proportional to a delayed glucose signal through a parameter called static β-cell responsivity (Φ_s). HE is assumed to be linearly related to plasma glucose concentration as in [24].

Model identification

The availability of the glucose fluxes in addition to plasma glucose, insulin and C-peptide concentrations, allowed identifying the model by using a system decomposition and forcing function strategy, paralleling what was done in [22]. This allowed us both to reduce the computational complexity of minimizing a six term objective function (including possible convergence to local minima) and avoid possible parameter miscompensation among the subsystems. Specifically, the model of *EGP* (A9)-(A11) was identified on *EGP*

data by using plasma glucose and insulin measurements as known (without error) inputs; the model of Ra_{meal} (A5)-(A8) was identified on Ra_{meal} data by using carbohydrate content of the meal as known input; the models described in (A1),(A12)-(A17) were identified simultaneously on plasma glucose and *U* data by using plasma insulin, *EGP* and Ra_{meal} as known inputs. The models reported in (A2)-(A4),(A18)-(A22) were identified on plasma C-peptide and insulin data by using plasma glucose and glucose rate of change as known inputs. Measurement error on Ra_{meal}, *EGP* and *U* was assumed to be independent, Gaussian, with zero mean and unknown constant SD. Measurement error on plasma glucose was assumed to be independent, Gaussian with zero mean and constant coefficient of variation (CV) of 2%. Errors on C-peptide and insulin measurements were assumed to be independent, Gaussian, with zero mean and variance dependent on the C-peptide and insulin measurements, respectively, as proposed in [30]. Measurement error on *EGP* and Ra_{meal} was assumed to be independent, Gaussian with zero mean and constant standard deviation *a posteriori* estimated, as previously described.

The parameter estimates, obtained from model identification in the 51 T2D subjects, were used to build up the joint parameter distribution, as described in the following section.

Estimation of the Joint Parameter Distribution

We observed that model parameters were lognormally distributed, thus the joint parameter distribution of T2D was univocally determined by the log-transformed average vector and covariance matrix of model parameters, named $\boldsymbol{\mu}_p$ and $\boldsymbol{\Sigma}_p$, respectively, which were calculated from parameter estimates as:

$$\boldsymbol{\mu}_p = \left[mean(\ln(p_1)), \dots, mean\left(\ln\left(p_{N_p}\right)\right)\right]^T \quad (1)$$

$$\boldsymbol{\Sigma}_p = \begin{bmatrix} var(\ln(p_1)) & \cdots & cov\left(\ln(p_1), \ln\left(p_{Np}\right)\right) \\ \vdots & \ddots & \vdots \\ cov\left(\ln\left(p_{Np}\right), \ln(p_1)\right) & \cdots & var\left(\ln\left(p_{Np}\right)\right) \end{bmatrix} \quad (2)$$

with N_p denoting the number of model parameters.

It is worth noting that, in principle, both $\boldsymbol{\mu}_p$ and $\boldsymbol{\Sigma}_p$ should be calculated using parameters estimated in the T2D subjects. However, while we were confident that the number of T2D subjects was sufficient to accurately calculate $\boldsymbol{\mu}_p$, we were unsure if this was the case for $\boldsymbol{\Sigma}_p$. Therefore, $\boldsymbol{\mu}_p$ was calculated using T2D parameters only, while $\boldsymbol{\Sigma}_p$ was calculated first by using only the parameters of the 51 T2D subjects, and then by merging the T2D and

healthy databases. The similarity between the two matrices was high, i.e., the distance (given by the norm of the difference between the two matrices) was small (1.497), proving that $\boldsymbol{\Sigma_p}$ was robust enough.

Generation and Assessment of the In Silico Population

As already stated, a key component of the simulator is the virtual population. Each virtual subject is represented by a vector of model parameters, **p:**

$$p = \left[p_1, p_2, \dots, p_{N_p}\right]^T \quad (3)$$

To generate the *in silico* population, one can randomly extract the desired number of **p** vectors from the joint parameter distribution described above.

To assess the adequacy of the generated *in silico* population, we compared the simulated plasma glucose, insulin and C-peptide concentrations in the generated T2D subjects with the data of [17]-[19]. For a fair comparison, we fed each *in silico* T2D subject with a CHO amount randomly sampled from a normal distribution $\mathcal{N}(\mu,\sigma)$, with μ=83.5g and σ=18.1g, equal to average and standard deviation of the CHO grams administered in the three studies, respectively. A graphical comparison was done by plotting the median and [5th-95th] percentile range of both simulated and real data; moreover, the glucose, insulin and C-peptide area under the curves (AUC) and time to peak (t_{peak}) were calculated for both simulations and measured data.

Case study

An interesting peculiarity of the simulator, besides well covering the average dynamics, lies in the possibility to evaluate the efficacy of a given treatment in rare, but not so rare, subjects. The following case study is presented to better grasp the potential of this simulation feature.

As case study, here we aim to assess if subjects with severe impairment in both insulin action and β-cell function (i.e., lowest k_{p3}, V_{mx}, Φ_d, Φ_s), denoted as $\overline{\mathrm{T2D}}$ may benefit from a double vs. a standard (i.e., single) dose of a hypothetical drug "X", designed to improve both insulin action and β-cell function (we assumed that the percentage increase in k_{p3}, V_{mx}, Φ_d and Φ_s was proportional to drug concentration). To do that, we run three *in silico* trials:

Diabetes Technology and Therapeutics
The Padova Type 2 Diabetes Simulator from Triple-Tracer Single Meal Studies: In Silico Trials also possible in Rare but Not-So-Rare Individuals (DOI: 10.1089/dia.2020.0110)

1. ISCT1: the entire T2D population (N=100) underwent two 7-hour meal tests (75 g of CHO), receiving X standard dose or no medication (NoMed), respectively;
2. ISCT2: the $\overline{\mathrm{T2D}}$ subjects underwent two 7-hour meal tests (75 g of CHO), receiving X standard dose or NoMed, respectively;
3. ISCT3: the $\overline{\mathrm{T2D}}$ subjects underwent two 7-hour meal tests (75 g of CHO), receiving X double dose or NoMed, respectively.

Statistical Analysis

Parameter estimates are presented as median [25^{th}-75^{th} percentile], and their precision expressed by the coefficient of variation (CV, defined as the ratio between the standard deviation of the estimated parameter and the estimated parameter value itself). Normally distributed metrics are reported as mean ± SD, while non-normally distributed ones as median [25^{th}-75^{th} percentile]. Normality was assessed with Lilliefors test. Statistical comparisons were performed by unpaired two-sample t-test or Wilcoxon rank sum test, for normal or non-normal distributions, respectively, with significance level $P = 0.05$.

RESULTS

Model fit and Parameter Estimates

The model well predicted glucose, insulin, C-peptide, *EGP*, Ra_{meal} and *U* data of T2D subjects, as proved by the weighted residuals shown in Fig. 3. Model parameters were estimated with good precision (numerical values are reported in Table A1,), with average CV = 31.9%. As expected, key parameters describing insulin action on glucose production and utilization (k_{p3} and V_{mx}) and β-cell responsiveness (Φ_s and Φ_d) resulted significantly lower ($P < 0.001$) than their counterparts obtained in healthy subjects [21]. Parameter distributions in T2D and H are shown in Fig. 4.

In Silico Population

A population of 100 *in silico* T2D subjects was generated. Simulated plasma glucose, insulin and C-peptide are compared with T2D data in Fig. 5. Results show a good agreement between simulations and data both in terms of population median and variability.

The glucose AUC was 6.9 [6.1-8.5] 10^4 mg/dL·min *in silico* vs. 7.0 [5.6-8.2] 10^4 mg/dL·min *in vivo*; time to peak was 88 [68-107] min *in silico* vs. 90 [75-113] min *in vivo*. The insulin AUC was 6.7 [5.2-9.7] 10^4 pmol/L·min *in silico* vs. 6.6 [4.4-10.1] 10^4 pmol/L·min *in vivo*; time to peak was 129 [109-168] min *in silico* vs. 120 [98-150] min *in vivo*. The C-peptide AUC was

749.0 ± 228.5 nmol/L·min *in silico* vs. 716.0 ± 250.8 nmol/L·min *in vivo*; time to peak was 162 [135-196] min *in silico* vs. 150 [120-180] min *in vivo*. No statistical significant differences were found in all the comparisons.

Case study

As shown in Fig. 6, in both the entire T2D and the $(T2D)^-$ population, the drug X has an effect in significantly improving postprandial glucose control compared to NoMed. However, X was not equally effective in the two groups. Distributions of AUC and tpeak calculated for glucose, insulin and C-peptide data are reported in Table 1.Drug effect on glucose regulation achieved in ISCT2,i.e.simulating standard dose of X in the $(T2D)^-$ subjects, was lower than that obtained in the entire T2D population (ISCT1): AUC percent difference was +14% (P = 0.028),+50% (P = 0.002),+19% (P = 0.037),for glucose, insulin and C-peptide, respectively. On the contrary, results achieved in ISCT3,i.e.simulating a double dose of X in the $(T2D)^-$, were statistically equivalent with those obtained in the entire population under standard X therapy: AUC percent difference was +7% (*P* = 0.218), +7% (*P* = 0.523), +9% (*P* = 0.318), for glucose, insulin and C-peptide, respectively.

DISCUSSION

A T2D simulator has been presented useful for testing diabetes treatments and for potentially accelerating the research needed to put on the market new antidiabetic drugs. The structure of the simulation model describing glucose regulation in T2D subjects is derived from that presented in [22], with an improved description of glucose kinetics in hypoglycemia [3], insulin kinetics and hepatic extraction [24], and C-peptide kinetics. Despite the importance of counterregulation in T2D, a mechanistic model of glucagon kinetics, secretion and action during a meal in T2D (and healthy) subjects is still lacking. We are working on such a model in an ongoing project and will incorporate it into the simulator as soon as results will become available.

An important aspect of this work is that the *in silico* T2D population was generated from a joint parameter distributions derived from T2D data. Indeed, the availability of plasma glucose, insulin C-peptide concentrations and of glucose fluxes coming from the studies [17]-[19] allowed us, for the first time, to identify the model on T2D subjects' data. However, we were unsure if the sample size (N=51) was sufficient to accurately assess parameter variability. Assuming that, despite differences in the average parameters, the

relationship between parameters was the same in T2D and H populations, we tested if deriving the distribution covariance matrix from T2D data only or from both H and T2D data would have significantly changed the results. This was not the case. An indirect prove of the validity of this assumption was also that the generated *in silico* T2D glucose, insulin and C-peptide concentrations very well matched the real one (Fig. 5).

The availability of 100 virtual subjects is important, since it allows running *in silico* large-scale trials, as usually occurs in phase II clinical trials. In addition, since virtual subjects can undergo the identical experimental scenario several times, one can implement an ideal crossover design, where physiological intra-subject variability is minimized (and controlled by the investigator).

Furthermore, the possibility to "virtually recruit" a subset of subjects with common characteristics, as shown in the proposed case study (Fig. 6), permits to extensively study situations characterized by "extreme" parameter vectors, sampled from the distribution tails. This could possibly be used for optimizing diabetes therapy also in such "rare" pathological conditions.

The domain of validity of the simulator is currently the single meal scenario. This might be a limitation for testing treatments that might have a different effect depending on time of administration. For example, long-acting insulin analogues might lead to a different glucose profile depending on morning or evening dosing, as already observed in T1D [31]. As a matter of fact, this work represents a proof of concept of a novel *in silico* strategy that allows one to evaluate treatments in T2D populations with certain characteristics. A future model refinement will include the description of intra-/inter-day variability of key model parameters, similarly to what has been recently done in H and T1D [32]-[34], thus improving the simulator reliability on long-term scenarios. In this regard, an ongoing study in T2D will provide important insights on intra- and inter-day variability of insulin sensitivity and beta-cell function [35].

In conclusion, we developed a simulation model describing glucose dynamics in T2D subjects. This is based on a large-scale model of glucose-insulin system and is equipped with an *in silico* population that reflect the main characteristics of T2D population. By allowing the evaluation of many treatment scenarios in a cost-effective way, the T2D simulator is usable for designing and testing new antidiabetic drugs.

ACKNOWLEDGMENTS

This work was supported by MIUR (Italian Minister for Education) under the initiative "Departments of Excellence" (Law 232/2016) and CARIPARO (Cassa di Risparmio di Padova e Rovigo) foundation under the initiative "Pediatric Research 2016-2018" (BCPD project). No potential conflicts of interest relevant to this article was reported. The authors thank Drs. Rita Basu, Andy Basu, Robert Rizza and Adrian Vella for let us use the T2D triple-tracer meal data set for developing the T2D simulator.

AUTHOR DISCLOSURE STATEMENT

All authors reviewed and approved the final version of the manuscript. R.V. built up the simulator, performed the simulations, contributed to the discussion and wrote the manuscript. C.C. conceived the model, contributed to interpretation of results and edited the manuscript. C.D.M. conceived the model, contributed to interpretation of results, edited the manuscript and is the guarantor of this work and, as such, had full access to all the data in the study and takes responsibility for the integrity of the data and the accuracy of the data analysis.

REFERENCES

[1] Viceconti M, Cobelli C, Haddad T, Himes A, Kovatchev B, Palmer M. In silico assessment of biomedical products: The conundrum of rare but not so rare events in two case studies. Proc Inst Mech Eng H. 2017;231(5):455-466. doi:10.1177/0954411917702931.

[2] Kovatchev BP, Breton M, Dalla Man C, Cobelli C. In Silico Preclinical Trials: A Proof of Concept in Closed-Loop Control of Type 1 Diabetes. J Diabetes Sci Technol. 2009;3(1):44-55. doi:10.1177/193229680900300106.

[3] Dalla Man C, Micheletto F, Lv D, Breton M, Kovatchev B, Cobelli C. The UVA/PADOVA Type 1 Diabetes Simulator: New Features. J Diabetes Sci Technol. 2014;8(1):26-34. doi

[4] Visentin R, Campos-Náñez E, Schiavon M, et al. The UVA/Padova Type 1 Diabetes Simulator Goes From Single Meal to Single Day. J Diabetes Sci Technol. 2018;12(2):273-281. doi:10.1177/1932296818757747.

[5] Toffanin C, Visentin R, Messori M, Palma F Di, Magni L, Cobelli C. Toward a Run-to-Run Adaptive Artificial Pancreas: In Silico Results. IEEE Trans Biomed Eng. 2018;65(3):479-488. doi:10.1109/TBME.2017.2652062.

[6] Toffanin C, Kozak M, Sumnik Z, Cobelli C, Petruzelkova L. In Silico Trials of an Open-Source Android-Based Artificial Pancreas: A New Paradigm to Test Safety and Efficacy of Do-It-Yourself Systems. Diabetes Technol Ther. 2020;22(2):112-120. doi:10.1089/dia.2019.0375.

[7] Shi D, Dassau E, Doyle FJ. Adaptive Zone Model Predictive Control of Artificial Pancreas Based on Glucose- and Velocity-Dependent Control Penalties. IEEE Trans Biomed Eng. 2019;66(4):1045-1054. doi:10.1109/TBME.2018.2866392.

[8] Garcia-Tirado J, Colmegna P, Corbett JP, Ozaslan B, Breton MD. In Silico Analysis of an Exercise-Safe Artificial Pancreas With Multistage Model Predictive Control and Insulin Safety System. J Diabetes Sci Technol. 2019;13(6):1054-1064. doi:10.1177/1932296819879084.

[9] Meneghetti L, Susto GA, Del Favero S. Detection of Insulin Pump Malfunctioning to Improve Safety in Artificial Pancreas Using Unsupervised Algorithms. J Diabetes Sci Technol. 2019;13(6):1065-1076. doi:10.1177/1932296819881452.

[10] Visentin R, Giegerich C, Jäger R, et al. Improving Efficacy of Inhaled Technosphere Insulin (Afrezza) by Postmeal Dosing: In-silico Clinical Trial with the University of Virginia/Padova Type 1 Diabetes Simulator. Diabetes Technol Ther. 2016;18(9):574-585. doi:10.1089/dia.2016.0128.

[11] Visentin R, Schiavon M, Giegerich C, Klabunde T, Dalla Man C, Cobelli C. Incorporating Long-Acting Insulin Glargine Into the UVA/Padova Type 1 Diabetes Simulator for In Silico Testing of MDI Therapies. IEEE Trans Biomed Eng. 2019;66(10):2889-2896. doi:10.1109/TBME.2019.2897851.

[12] Schiavon M, Visentin R, Giegerich C, Sieber J, Cobelli C, Dalla Man C, Klabunde T. *In Silico* Head-to-Head Comparison of Insulin Glargine 300 U/mL and Insulin Degludec 100 U/mL in Type 1 Diabetes. Diabetes Technol Ther. 2020 ahead of print. doi:10.1089/dia.2020.0027.

[13] Vettoretti M, Facchinetti A, Sparacino G, Cobelli C. Type-1 Diabetes Patient Decision Simulator for In Silico Testing Safety and Effectiveness of Insulin Treatments. IEEE Trans Biomed Eng. 2018;65(6):1281-1290. doi:10.1109/TBME.2017.2746340

[14] Edelman S V. Regulation Catches Up to Reality. J Diabetes Sci Technol. 2017;11(1):160-164. doi:10.1177/1932296816667749.

[15] Tran L, Zielinski A, Roach AH, et al. Pharmacologic Treatment of Type 2 Diabetes: Oral Medications. Ann Pharmacother. 2015;49(5):540-556. doi:10.1177/1060028014558289.

[16] Tran L, Zielinski A, Roach AH, et al. Pharmacologic Treatment of Type 2 Diabetes: Injectable Medications. Ann Pharmacother. 2015;49(6):700-714. doi:10.1177/1060028015573010.

[17] Bock G, Dalla Man C, Campioni M, et al. Pathogenesis of pre-diabetes: Mechanisms of fasting and postprandial hyperglycemia in people with impaired fasting glucose and/or impaired glucose tolerance. Diabetes. 2006;55(12):3536-3549. doi:10.2337/db06-0319.

[18] Vella A, Bock G, Giesler PD, et al. Effects of Dipeptidyl Peptidase-4 Inhibition on Gastrointestinal Function, Meal Appearance, and Glucose Metabolism in Type 2 Diabetes. Diabetes. 2007;56(5):1475 LP - 1480. doi:10.2337/db07-0136.

[19] Basu A, Dalla Man C, Basu R, Toffolo G, Cobelli C, Rizza RA. Effects of type 2 diabetes on insulin secretion, insulin action, glucose effectiveness, and postprandial glucose metabolism. Diabetes Care. 2009;32(5):866-872. doi:10.2337/dc08-1826.

[20] Basu R, Di Camillo B, Toffolo G, et al. Use of a novel triple-tracer approach to assess postprandial glucose metabolism. Am J Physiol Endocrinol Metab. 2003;284(1):E55-69. doi:10.1152/ajpendo.00190.2001.

[21] Basu R, Dalla Man C, Campioni M, et al. Effects of age and sex on postprandial glucose metabolism differences in glucose turnover, insulin secretion, insulin action, and hepatic insulin extraction. Diabetes. 2006;55(7):2001-2014. doi:10.2337/db05-1692.

[22] Dalla Man C, Rizza RA, Cobelli C. Meal simulation model of the glucose-insulin system. IEEE Trans Biomed Eng. 2007;54(10):1740-1749. doi:10.1109/TBME.2007.893506.

[23] Sherwin RS, Kramer KJ, Tobin JD, et al. A model of the kinetics of insulin in man. J Clin Invest. 1974;53(5):1481-1492. doi:10.1172/JCI107697.

[24] Piccinini F, Dalla Man C, Vella A, Cobelli C. A Model for the Estimation of Hepatic Insulin Extraction after a Meal. IEEE Trans Biomed Eng. 2016;63(9):1925-1932. doi:10.1109/TBME.2015.2505507.

[25] Eaton RP, Allen RC, Schade DS, Erickson KM, Standefer J. Prehepatic insulin production in man: kinetic analysis using peripheral connecting peptide behavior. J Clin Endocrinol Metab. 1980;51(3):520-528. doi:10.1210/jcem-51-3-520.

[26] Van Cauter E, Mestrez F, Sturis J, Polonsky KS. Estimation of insulin secretion rates from C-peptide levels: Comparison of individual and standard kinetic parameters for C-peptide clearance. Diabetes. 1992;41(3):368-377. doi:10.2337/diabetes.41.3.368.

[27] Dalla Man C, Toffolo G, Basu R, Rizza RA, Cobelli C. A model of glucose production during a meal. Annu Int Conf IEEE Eng Med Biol - Proc. 2006;0(0):5647-5650. doi:10.1109/IEMBS.2006.260809.

[28] Dalla Man C, Camilleri M, Cobelli C. A system model of oral glucose absorption: Validation on gold standard data. IEEE Trans Biomed Eng. 2006;53(12):2472-2478. doi:10.1109/TBME.2006.883792.

[29] Yki-Jarvinen H, Young AA, Lamkin C, Foley JE. Kinetics of glucose disposal in whole body and across the forearm in man. J Clin Invest. 1987;79(6):1713-1719. doi:10.1172/JCI113011.

[30] Toffolo G, Campioni M, Basu R, Rizza R a, Cobelli C. A minimal model of insulin secretion and kinetics to assess hepatic insulin extraction. Am J Physiol Endocrinol Metab. 2006;290(1):E169-E176. doi:10.1152/ajpendo.00473.2004.

[31] Bergenstal RM, Bailey TS, Rodbard D, et al. Comparison of Insulin Glargine 300 Units/mL and 100 Units/mL in Adults With Type 1 Diabetes: Continuous Glucose Monitoring Profiles and Variability Using Morning or Evening Injections. Diabetes Care. 2017;40(4):554-560. doi:10.2337/dc16-0684.

[32] Saad A, Dalla Man C, Nandy DK, et al. Diurnal pattern to insulin secretion and insulin action in healthy individuals. Diabetes. 2012;61(11):2691-2700. doi:10.2337/db11-1478.

[33] Hinshaw L, Dalla Man C, Nandy DK, et al. Diurnal pattern of insulin action in type 1 diabetes implications for a closed-Loop system. Diabetes. 2013;62(7):2223-2229. doi:10.2337/db12-1759.

[34] Visentin R, Dalla Man C, Kudva YC, Basu A, Cobelli C. Circadian Variability of Insulin Sensitivity: Physiological Input for In Silico Artificial Pancreas. Diabetes Technol Ther. 2015;17(1):1-7. doi:10.1089/dia.2014.0192.

[35] Romeres D, Schiavon M, Cobelli C, Dalla Man C, Basu A, Basu R. 224-OR: Diurnal Pattern of Insulin Action and Beta-Cell Function in Health and Type 2 Diabetes. Diabetes. 2019;68(Supplement 1):224-OR. doi:10.2337/db19-224-OR.

APPENDIX

Model Equations

Glucose Kinetics:

$$\begin{cases} \dot{G}_p(t) = EGP(t) + Ra_{meal}(t) - U_{ii}(t) - E(t) - k_1 G_p(t) + k_2 G_t(t) & G_p(0) = \\ \dot{G}_t(t) = -U_{id}(t) + k_1 G_p(t) - k_2 G_t(t) & G_t(0) = \\ G(t) = G_p(t)/V_G & G(0) = \end{cases} \quad \text{(A1)}$$

where G_p and G_t (mg/kg) are glucose masses in plasma and rapidly equilibrating and in slowly equilibrating tissues, respectively; G (mg/dL) is the plasma glucose concentration; suffix b denotes basal state; EGP is the endogenous glucose production (mg/kg/min); Ra_{meal} is the glucose rate of appearance in plasma (mg/kg/min); E is renal excretion (mg/kg/min); U_{ii} and U_{id} (mg/kg/min) are the insulin-independent and insulin-dependent glucose utilizations, respectively. The description of model parameters is provided in Table A1 – *Glucose Kinetics*.

Insulin Kinetics:

$$\begin{cases} \dot{I}_l(t) = -\big(m_1 + m_3(t)\big) I_l(t) + m_2 I_p(t) + ISR(t)/BW & I_l(0) = I_{lb} \\ \dot{I}_p(t) = -(m_2 + m_4 + m_5) I_p(t) + m_1 I_l(t) + m_6 I_{ev}(t) & I_p(0) = I_{pb} \\ \dot{I_{ev}}(t) = -m_6 I_{ev}(t) + m_5 I_p(t) & I_{ev}(0) = I_{evb} \\ I(t) = I_p(t)/V_I & I(0) = I_b \end{cases} \quad \text{(A2)}$$

with

$$m_3(t) = \frac{HE(t) \cdot m_1}{1 - HE(t)} \quad \text{(A3)}$$

$$HE(t) = -a_G \cdot G(t) + a_{0G} \quad \text{(A4)}$$

where I_l, I_p and I_{ev} (pmol/kg) are insulin masses in plasma, liver and extravascular space, respectively; I (pmol/L) is the plasma insulin concentration; suffix b denotes basal state; ISR (pmol/min) is the beta-cell insulin (and C-peptide) secretion rate; HE (dimensionless) is the hepatic extraction. The description of model parameters is provided in Table A1 – *Insulin Kinetics*.

Rate of Glucose Appearance:

$$\begin{cases} Q_{sto}(t) = Q_{sto1}(t) + Q_{sto2}(t) & Q_{sto}(0) = 0 \\ \dot{Q}_{sto1}(t) = -k_{max}Q_{sto1}(t) + Dose \cdot \delta(t) & Q_{sto1}(0) = 0 \\ \dot{Q}_{sto2}(t) = -k_{empt}(Q_{sto})Q_{sto2}(t) + k_{max}Q_{sto1}(t) & Q_{sto2}(0) = 0 \\ \dot{Q}_{gut}(t) = -k_{abs}Q_{gut}(t) + k_{empt}(Q_{sto})Q_{sto2}(t) & Q_{gut}(0) = 0 \\ Ra_{meal}(t) = \dfrac{f \cdot k_{abs}Q_{gut}(t)}{BW} & Ra_{meal}(0) = 0 \end{cases} \quad \text{(A5)}$$

with

$$k_{empt}(Q_{sto}) = k_{min} + \frac{k_{max} - k_{min}}{2} \cdot \{\tanh[\alpha(Q_{sto} - \beta \cdot Dose)] - \tanh[\beta(Q_{sto} - c \cdot Dose)] + 2\} \quad \text{(A6)}$$

$$\alpha = \frac{5}{2 \cdot Dose \cdot (1 - b)} \quad \text{(A7)}$$

$$\beta = \frac{5}{2 \cdot Dose \cdot d} \quad \text{(A8)}$$

where Q_{sto} (mg) is the amount of glucose in the stomach (solid, Q_{sto1} and liquid phase Q_{sto2}); Q_{gut} (mg) is the glucose mass in the intestine; *Dose* (mg) is the amount of ingested glucose; *BW* (kg) is the body weight. The description of model parameters is provided in Table A1 – *Rate of Glucose Appearance*.

Endogenous Glucose Production:

$$EGP(t) = k_{p1} - k_{p2}G_p(t) - k_{p3}X^L(t) - k_{p4}I_l(t) \quad \text{(A9)}$$

$$\dot{X}^L(t) = -k_i \cdot [X^L(t) - I'(t)] \quad X^L(0) = I_b \quad \text{(A10)}$$

$$\dot{I}'(t) = -k_i \cdot [I'(t) - I(t)] \quad I'(0) = I_b \quad \text{(A11)}$$

where X^L (pmol/L) is the delayed insulin action (through intermediate compartment I'); I_l (pmol/kg) is insulin mass in the liver; I (pmol/L) is plasma insulin concentration; suffix b denotes basal state. The description of model parameters is provided in Table A1 – *Endogenous Glucose Production*.

Glucose Utilization:

$$U_{ii}(t) = F_{cns} \quad \text{(A12)}$$

$$U_{id}(t) = \frac{[V_{m0} + V_{mx} \cdot X(t) \cdot (1 + r_1 \cdot risk)] \cdot G_t(t)}{K_{m0} + G_t(t)} \quad \text{(A13)}$$

with

$$\dot{X}(t) = -p_{2u} \cdot X(t) + p_{2u} \cdot [I(t) - I_b] \quad X(0) = 0 \tag{A14}$$

$$risk = \begin{cases} 0 & if\ G \geq G_b \\ 10 \cdot [f(G)]^2 & if\ G_{th} \leq G \leq G_b \\ 10 \cdot [f(G_{th})]^2 & if\ G \leq G_{th} \end{cases} \tag{A15}$$

$$f(G) = [\log(G)]^{r_2} - [\log(G_b)]^{r_2} \tag{A16}$$

where U_{ii} and U_{id} (mg/kg/min) are the insulin-independent and insulin-dependent utilization, respectively; X (pmol/L) is the insulin action on glucose utilization; G_t (mg/kg) is glucose mass in the tissues; G (mg/dL) is plasma glucose concentration; suffix *b* denotes basal state. The description of model parameters is provided in Table A1 – *Glucose Utilization*.

Renal Excretion:

$$E(t) = \begin{cases} k_{e1} \cdot \left[G_p(t) - k_{e2}\right] & if\ G_p(t) > k_{e2} \\ 0 & if\ G_p(t) \leq k_{e2} \end{cases} \tag{A17}$$

where E (mg/kg/min) is the renal excretion; G_p (mg/kg) is glucose mass in plasma. The description of model parameters is provided in Table A1 – *Renal Excretion*.

C-peptide Kinetics:

$$\begin{cases} \dot{CP_1}(t) = -(k_{01} + k_{21})CP_1(t) + k_{12}CP_2(t) + ISR(t)/V_c & CP_1(0) = CP_b \\ \dot{CP_2}(t) = -k_{12}CP_2(t) + k_{21}CP_1(t) & CP_2(0) = \dfrac{k_{21}}{k_{12}}CP_b \end{cases} \tag{A18}$$

where CP_1 and CP_2 (pmol/L) are C-peptide concentrations in the accessible and in the peripheral compartment; suffix *b* denotes basal state. The description of model parameters is provided in Table A1 – *C-peptide Kinetics*.

Insulin and C-peptide Secretion:

$$ISR(t) = ISR_s(t) + ISR_d(t) + ISR_b(t) \tag{A19}$$

$$\dot{ISR_s}(t) = -\alpha \cdot [ISR_s(t) - V_c \cdot \Phi_s \cdot (G(t) - h)] \quad ISR_s(0) = 0 \tag{A20}$$

$$ISR_d(t) = \begin{cases} V_c \cdot \Phi_d \cdot \dot{G}(t) & if\ \dot{G}(t) \geq 0 \\ 0 & if\ \dot{G}(t) < 0 \end{cases} \tag{A21}$$

$$ISR_b(t) = CP_b \cdot k_{01} \cdot V_c \tag{A22}$$

where ISR, ISR_s, ISR_d, and ISR_b (pmol/min) are the total, static, dynamic and basal components, respectively of the C-peptide (and insulin) secretion rates from the beta-cells; G (mg/dL) is plasma glucose concentration; suffix *b* denotes basal state. The description of model parameters is provided in Table A1 – *Insulin and C-peptide Secretion*.

Diabetes Technology and Therapeutics
The Padova Type 2 Diabetes Simulator from Triple-Tracer Single Meal Studies: In Silico Trials also possible in Rare but Not-So-Rare Individuals (DOI: 10.1089/dia.2020.0110)

Table 1. Case study metrics

		AUC	t_{peak}
Glucose	T2D – NoMed	8.3 [7.3-9.8]	88 [71-109]
	T2D – X_{single}	6.7 [6.0-8.1]*	63 [53-74]*
	$\overline{T2D}$ – NoMed	10.4 [8.7-11.1]	95 [88-114]
	$\overline{T2D}$ – X_{single}	8.4 [7.5-8.8]§	73 [61-78]§
	$\overline{T2D}$ – X_{double}	7.5 [7.1-8.3]§	55 [51-62]§
Insulin	T2D – NoMed	7.2 [5.6-9.4]	130 [106-167]
	T2D – X_{single}	5.9 [4.3-7.5]*	96 [80-117]*
	$\overline{T2D}$ – NoMed	11.3 [8.5-13.9]	151 [126-171]
	$\overline{T2D}$ – X_{single}	9.0 [7.0 10.5]§	106 [96-128]§
	$\overline{T2D}$ – X_{double}	6.0 [5.3-7.3]	86 [82-92]
C-peptide	T2D – NoMed	820.1 [711.2-936.7]	161 [136-197]
	T2D – X_{single}	725.5 [621.0-849.2]*	119 [104-139]*
	$\overline{T2D}$ – NoMed	930.6 [769.7-979.5]	191 [162-212]
	$\overline{T2D}$ – X_{single}	875.6 [708.8-935.7]	132 [120-157]§
	$\overline{T2D}$ – X_{double}	662.0 [535.5-722.0]§	110 [96-122]§

Distribution of glucose, insulin and C-peptide AUC and t_{peak}, calculated in the entire T2D population (N=100) and in the 10 most impaired T2D subjects ($\overline{(T2D)}$) with no medication (NoMed) or treated with drug X with single (Xsingle) or double (Xdouble) dose.Values are reported as median [25th-75th percentile].*P<0.01 from paired Wilcoxon signed rank test against T2D - NoMed.§: P<0.01 from paired Wilcoxon signed rank test against $\overline{(T2D)}$ - NoMed.

Diabetes Technology and Therapeutics
The Padova Type 2 Diabetes Simulator from Triple-Tracer Single Meal Studies: In Silico Trials also possible in Rare but Not-So-Rare Individuals (DOI: 10.1089/dia.2020.0110)
This paper has been peer-reviewed and accepted for publication, but has yet to undergo copyediting and proof correction. The final published version may differ from this proof.

Table A1. Parameter estimates

Process	*Parameter*	*Description and Unit*	*T2D*
Glucose Kinetics	V_G	*distribution volume (dL/kg)*	1.00 [0.73-1.33]
	k_1	*rate parameter (min^{-1})*	0.066 [0.053-0.073]
	k_2	*rate parameter (min^{-1})*	0.043 [0.020-0.072]
Insulin Kinetics	V_I	*distribution volume (L/kg)*	0.041 [0.039-0.062]
	m_1	*rate parameter (min^{-1})*	0.314 [0.245-1.812]
	m_2	*rate parameters (min^{-1})*	*fixed to 0.268 based on* [23]
	m_4	*rate parameter (min^{-1})*	0.443 [0.299-0.617]
	m_5	*rate parameter (min^{-1})*	0.260 [0.057-0.420]
	m_6	*rate parameter (min^{-1})*	0.017 [0.011-0.021]
	HE_b	*basal hepatic insulin extraction (dimensionless)*	*derived from* (A2) *steady-state*
	a_G	*glucose control on HE (dL/mg)*	0.005 [0.003-0.008]
	a_{0G}	*extrapolated HE at zero glucose (dimensionless)*	*derived from* (A4) *at steady-state*
Rate of Glucose Appearance	k_{abs}	*rate constant of intestinal absorption (min^{-1})*	0.0542 [0.0293-0.1000]
	k_{max}	*maximum gastric emptying rate (min^{-1})*	0.0426 [0.0318-0.0869]
	k_{min}	*minimum gastric emptying rate (min^{-1})*	0.0076 [0.0066-0.0100]
	b	*inflection point of gastric emptying curve (dimensionless)*	0.73 [0.58-0.83]
	d	*inflection point of gastric emptying curve (dimensionless)*	0.10 [0.06-0.14]
	f	*fraction of intestinal absorption (dimensionless)*	*fixed to 0.9 based on* [22]

Endogenous Glucose Production	k_{p1}	*extrapolated EGP at zero glucose and insulin (mg/kg/min)*	*derived from* (A9) *at steady-state*
	k_{p2}	*hepatic glucose effectiveness (min^{-1})*	0.0008 [0.0007-0.0036]
	k_{p3}	*hepatic insulin sensitivity (mg/kg/min per pmol/L)*	0.0060 [0.0046-0.0085]
	k_{p4}	*portal insulin sensitivity (mg/kg/min per pmol/kg)*	0.0484 [0.0333-0.0656]
	k_i	*rate of delayed insulin action (min^{-1})*	0.0075 [0.0056-0.0101]
Glucose Utilization	F_{cns}	*insulin-independent glucose utilization (mg/kg/min)*	*fixed to 1 based on* [22]
	V_{mx}	*insulin sensitivity on glucose utilization (mg/kg/min per pmol/L)*	0.034 [0.020-0.055]
	K_{m0}	*glucose mass appearing in Michaelis-Menten relation (mg/kg)*	466.2 [362.5-511.1]
	p_{2U}	*rate of insulin action on glucose utilization (min^{-1})*	0.058 [0.025-0.097]
	r_1, r_2	*parameters of risk function (dimensionless)*	*fixed to values as proposed in* [3]
Renal Excretion	k_{e1}	*glomerular filtration rate (min^{-1})*	*fixed to 0.0005 based on* [22]
	k_{e2}	*renal threshold of glucose (mg/kg)*	*fixed to 339 based on* [22]
C-peptide Kinetics	V_C	*distribution volume (L)*	*fixed to standard population values as proposed in* [26]
	k_{01}, k_{12}, k_{21}	*rate parameters (min^{-1})*	*fixed to standard population values as proposed in* [26]
Insulin &	α	*delay between glucose and insulin*	0.034 [0.023-0.041]

C-peptide Secretion		*secretion (min^{-1})*	
	Φ_s	*β-cell responsivity to glucose (10^{-9} min^{-1})*	20.30 [12.51-28.03]
	Φ_d	*β-cell responsivity to glucose rate of change (10^{-9})*	286.0 [148.6-404.6]
	h	*glucose threshold on β-cells secretion (mg/dL)*	98.7 [75.6-133.2]

Distribution of estimated model parameters obtained from T2D data (N=51). Values are reported as median [25^{th}-75^{th} percentile].

Diabetes Technology and Therapeutics
The Padova Type 2 Diabetes Simulator from Triple-Tracer Single Meal Studies: In Silico Trials also possible in Rare but Not-So-Rare Individuals (DOI: 10.1089/dia.2020.0110)

FIGURE LEGENDS

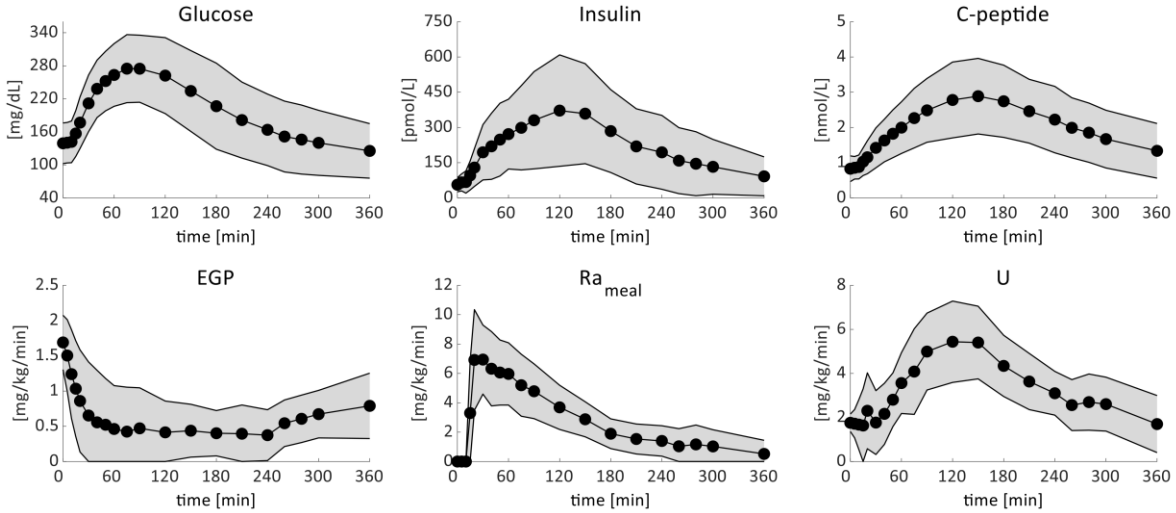

Figure 1: Average (filled circle) ± standard deviation (SD, shaded area) plasma glucose, insulin and C-peptide concentration (*upper*) and estimated endogenous glucose production (*EGP*), glucose rate of appearance (Ra_{meal}) and glucose utilization (*U*) (*lower panels*) in T2D subjects (N=51).

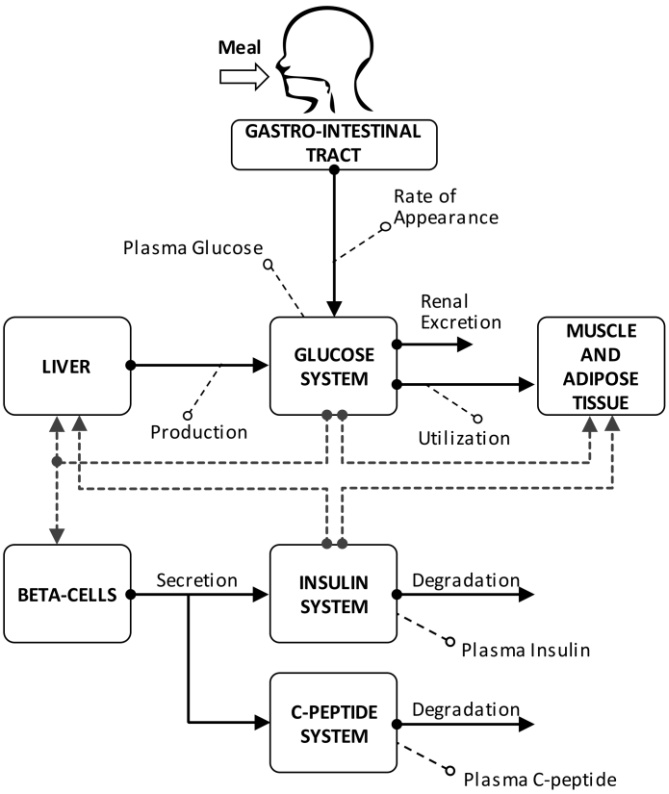

Figure 2: Scheme of the T2D simulation model. Metabolic fluxes are indicated with continuous lines, while control actions are represented by dashed lines.

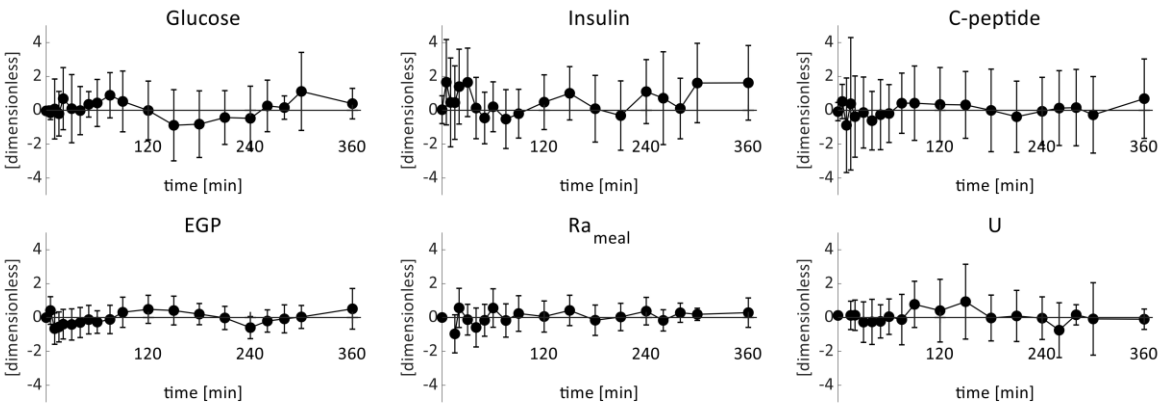

Figure 3: Average weighted residuals [vertical bars represent standard deviation (SD)] of model fit on plasma glucose, insulin, C-peptide, *EGP*, Ra_{meal} and *U* in T2D subjects (N=51).

Diabetes Technology and Therapeutics
The Padova Type 2 Diabetes Simulator from Triple-Tracer Single Meal Studies: In Silico Trials also possible in Rare but Not-So-Rare Individuals (DOI: 10.1089/dia.2020.0110)
This paper has been peer-reviewed and accepted for publication, but has yet to undergo copyediting and proof correction. The final published version may differ from this proof.

Diabetes Technology and Therapeutics
The Padova Type 2 Diabetes Simulator from Triple-Tracer Single Meal Studies: In Silico Trials also possible in Rare but Not-So-Rare Individuals (DOI: 10.1089/dia.2020.0110)
This paper has been peer-reviewed and accepted for publication, but has yet to undergo copyediting and proof correction. The final published version may differ from this proof.

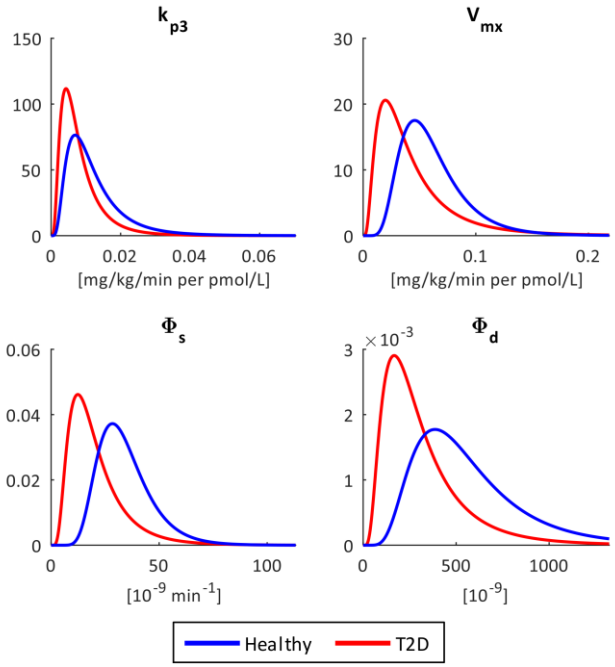

Figure 4: Distribution of insulin sensitivity parameters, V_{mx} and k_{p3} (*upper panels*), and β-cell responsivity indices, Φ_s and Φ_d (*lower panels*), estimated in T2D (red lines, N = 51) and healthy subjects of [21] (blue lines, N = 204).

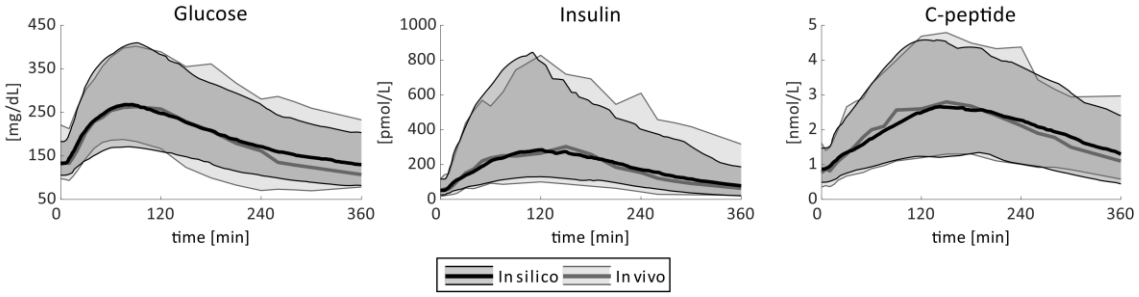

Figure 5: Plasma glucose (*left*), insulin (*center*) and C-peptide (*right panel*) concentrations in *in silico* (dark gray area and black line) vs. *in vivo* (light gray area and gray line). Time courses are shown as median (thick line) and [5%-95%] range (shaded area).

Diabetes Technology and Therapeutics
The Padova Type 2 Diabetes Simulator from Triple-Tracer Single Meal Studies: In Silico Trials also possible in Rare but Not-So-Rare Individuals (DOI: 10.1089/dia.2020.0110)

Diabetes Technology and Therapeutics
The Padova Type 2 Diabetes Simulator from Triple-Tracer Single Meal Studies: In Silico Trials also possible in Rare but Not-So-Rare Individuals (DOI: 10.1089/dia.2020.0110)

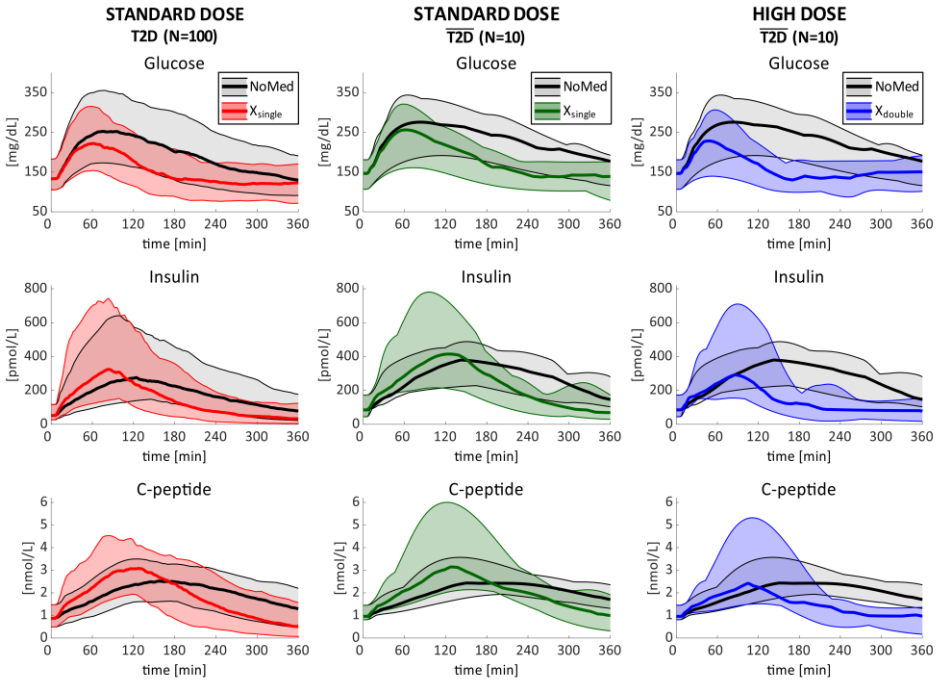

Figure 6: *In silico* plasma glucose (*upper*), insulin (*middle*) and C-peptide (*lower panels*) obtained by simulating ISCT1 (i.e., single dose of X in the entire T2D population, red area and line, *left*), ISCT2 (i.e., single dose of X in the $\overline{\text{T2D}}$ subjects, green area and line, *center*), ISCT3 (i.e., double dose of X in the $\overline{\text{T2D}}$ subjects, blue area and line, *right panels*) vs. no medication (NoMed, light gray area and gray line). Time courses are shown as median (thick lines) and [5%-95%] range (shaded areas).